

Research Article

Grouting Mechanism in Water-Bearing Fractured Rock Based on Two-Phase Flow

Bo Ren ^{1,2} **Wenqiang Mu** ³ **Bingyou Jiang** ⁴ **Guofeng Yu**,^{2,4} **Lianchong Li** ³
Tingshuang Wei,⁵ **Yunchun Han**,² and **Diancai Xiao**²

¹*School of Emergency Management and Safety Engineering, China University of Mining and Technology (Beijing), Beijing 100083, China*

²*State Key Laboratory of Deep Coal Mining & Environment Protection, Coal Mining National Engineering Technology Research Institute, Huainan 232000, China*

³*School of Resources and Civil Engineering, Northeastern University, Shenyang 110819, China*

⁴*School of Energy and Safety, Anhui University of Science and Technology, Huainan 232001, China*

⁵*Coal Industry Branch of Huaihe Energy Group, Huainan 232000, China*

Correspondence should be addressed to Wenqiang Mu; neumwq2017@163.com and Bingyou Jiang; 15955413831@163.com

Received 7 January 2021; Revised 27 January 2021; Accepted 29 January 2021; Published 25 February 2021

Academic Editor: Feng Xiong

Copyright © 2021 Bo Ren et al. This is an open access article distributed under the Creative Commons Attribution License, which permits unrestricted use, distribution, and reproduction in any medium, provided the original work is properly cited.

Grouting is always used in mine water plugging, reinforcement, and other disaster prevention projects. The diffusion mechanism of slurry in fractured rock is affected by geological environment and slurry performance, which should be revealed and characterized better. Based on the two-phase flow diffusion theory, a slurry diffusion model considering flowing water condition was established for a blocking area of a fracture zone in one case from China. The feasibility of two-phase flow model in grouting diffusion calculation was analyzed. The diffusion model in dynamic water environment was studied, and the diffusion range varying with time in the grouting area of Zhangji Coal Mine was explored. The optimization method of multi grouting holes was put forward, and the influence of water flowing was discussed. The results show that the slurry diffusion calculated by the two-phase flow model was feasible and consistent with the experimental study. The dynamic water can change the conventional circular diffusion state of slurry, but its pattern was oval and leaf type. There were different penetration distances in directions, and typical grouting voids were made on the side and upstream. When the single-hole grouting was carried out, the predetermined value can be achieved in the height range, but it was only about 15 m on the side because of the water flowing, which cannot meet the requirements. The optimization scheme of grouting was put forward, which adopted multiple grouting holes in the long side, and grouting in different directions and periods to avoid the possible problems of multihole intersection. The rationality and effectiveness of the proposed optimization method were verified through the calculation of water yield and analysis of cement composition from the drilling core in the grouted zone. In the grouting process, the water flowing has double effects, which has a significant role in promoting and scouring along the flow direction, but there is a significant weakness in the side diffusion. It is very important to realize the rational use of the dynamic water through the optimization scheme. This study is an important basic work of grouting mechanism, and it is expected to promote the development of grouting technology and application of two-phase fluid-solid coupling theory.

1. Introduction

As one of the main energy resources, coal is widely used in power generation, heating, steel, and other industrial production. China is very dependent on coal energy with the geological conditions of more coal and less oil. Considering the

higher efficiency and exhaustion of resources, coal mining tends to be mined in depth and is limited by the complex geological conditions and mining technologies, accidents such as rock-burst, gas explosion, water inrush, and roof fall occur frequently [1–5], which seriously threaten the production safety. Therefore, corresponding prevention and control

measures must be taken to keep mining, such as forced caving, gas drainage, and bolt-grouting [6, 7]. To govern the geological fractures, grouting has been widely used in mining engineering, tunnel engineering, and other major construction projects [8–10]. The grouting process is to inject cement or other slurries into the structure with injection bolts, which will block the fractures and cement broken bodies to achieve sealing and reinforcement [11]. Especially in the mine threatened by the floor confined water, the comprehensive method of grouting and drainage become the key technology to ensure the safety of mining production. Therefore, the grouting equipment, materials, and their flow mechanism have been deeply studied [12–15].

Grouting engineering is a continuous and complex procedure. In the fractures, the slurry is driven by the external pressure and diffuses. The diffusion range is the key to ensure its quality, which is affected by the properties of slurry, flow channels, and geological matrix [16]. Grouting slurry shows the various fluid with different hydraulic properties and is suitable for different construction conditions [17–19]. To meet the needs of high-quality engineering, many chemical slurries have been developed to prevent leakage, which is generally characterized by Newtonian fluid. However, cement is often used in the water plugging in coal mining. The flow characteristics of cement are related to temperature and water-cement ratio (w/c), which can be divided into Newtonian fluid ($w/c > 1.0$), Bingham fluid ($1.0 > w/c > 0.7$), and power-law fluid ($0.7 > w/c$) [20, 21]. The flow pattern of the slurry plays a key role in the diffusion, which must be considered in the grouting calculation. The cement slurry of Newtonian type is always used in the coal mine to seal the fractures to water plugging completely, which can be injected into the fractured zone with grouting equipment. Therefore, the diffusion process of Newtonian grout in cracks has been widely studied, but further research is needed to meet the engineering needs [15, 22].

The conventional research is to calculate the parameters of a single slurry fluid by the Navier-Stokes equation (NS equation) and Darcy's law, which can be used to estimate the actual engineering consumption [23–25]. It is difficult to meet the actual needs of grouting process with parameters calculated by conventional simple formula. Therefore, the research on grouting mechanism and method still needs to be carried out in depth. As the basis of grouting construction and research, many researches have been carried out on the slurry diffusion of single-plane fracture. The pressure distribution and final range of slurry diffusion in the fracture were derived with the simplified fracture of a two-dimensional smooth and nondeformable one by Wittke and Wallner [26]. Funehag and Gustafson developed a penetration model of one-dimensional grouting flow in the channel with the simplified parameters as to calculate the penetration length of silica sol [27]. El Tani and Stille simplified the silicon solution and cemented grouting as a channel flow in the plane fracture, analyzed the flow of silicon dioxide solution and cement with the Bingham type under the Gin method, and established a systematic representation of the analytical relationship between grouting diffusion and time period [12]. Based on the common rheological Bingham model, Funehag

and Thörn studied grouting diffusion in a single fracture [28]. In order to truly reflect and simulate the actual situation of the site, the complexity, crisscross, and undulation of geological fractures are considered in grouting calculation. Mu et al. studied the influence of roughness, dip angle, and coupling degree on slurry diffusion based on a single rough fracture model [29]. Yang et al. simulated the fracture of single rough rock in the tunnel with the self-designed simulation device [30]. The numerical simulation of the slurry diffusion process in a single-slab fracture without external environment interference can be carried out. The research content can promote the application and development of grouting technology in engineering. However, the accurate characterization of slurry diffusion range, especially considering the external environment, such as water flowing, still needs further studies.

The external environment of grouting is complex, in which the grouting is often carried out for the water blocking, so there is obvious dynamic water interference in the grouting process, and many studies have been carried out in depth. Based on the experiment, Sui et al. established the slurry diffusion model in the single-plane fracture with the effects of dynamic water and studied the distribution characteristics of sealing effect under the condition of water flow [31]. Yang et al. analyzed the influence of multiple factors on slurry diffusion and sealing performance in view of fracture grouting diffusion in water environment [32, 33]. Wang et al. pointed out that the slurry penetration under flowing water has spatial heterogeneity and the mechanical behavior of slurry under water washing was studied by constructing a rough rock fracture model [34]. Guo et al. established the theoretical model of fracture flow grouting, deduced the streamline equation of grouting diffusion trajectory with flowing water based on considering the boundary conditions, and analyzed the influence of boundary effect on grouting diffusion law [35]. Liu et al. simulated the flowing water grouting process in rough rock fractures through a series of physical simulation tests and studied the influence of slurry composition content on grouting fluid pressure and plugging effect [36]. Water flow has an important influence on the hydraulic characteristics such as the pressure distribution and permeability of the slurry in the fracture [37]. When the cement slurry blocks the water flow, the water flow also has multiple effects on the cement slurry, such as scouring, dilution, and promoting diffusion. The accurate characterization of this process is of great significance to optimize the grouting process and design.

There are significant differences in properties and flow patterns between cement slurry and water. It is not a single-fluid diffusion of slurry, but a process of slurry displacing fracture water flow. Therefore, the slurry diffusion can be regarded as a two-phase flow process of slurry and water. For the two-phase flow theory, there are two ways to track the two-phase flow interface: the level set method and phase field method [38]. Using these two methods, we can get the proportion of the two kinds of fluid in the calculation domain and get the corresponding hydraulic parameters. Then the two-phase driven diffusion of slurry and water can be solved by the level set method. Through this method, the effective

diffusion characteristics of cement under the action of water flow, especially under the condition of flowing water, can be obtained [37]. The results obtained by tracing the diffusion boundary of two-phase flow can be used to analyze the influence of crack boundary, water velocity, and other factors on grouting. At the same time, corresponding solutions can be put forward for different situations to meet the needs of the actual project.

Based on the N-S flow equation and the two-phase flow level set method, the research work is carried out in this paper. COMSOL is used to build the diffusion model of slurry in fracture, and the diffusion characteristics of slurry in dynamic water are studied based on CFD module. Combined with the diffusion characteristics of engineering scale, the corresponding solutions are proposed to better meet the needs of mining engineering.

2. Engineering Case

2.1. Mining and Geological Conditions. The present analysis was based on the mining and geological conditions of Zhangji Coal Mine in Huainan city in Panxie mining area of China, as shown in Figure 1. The mine is divided into two levels and 20 mining areas. The mine is concentrated in the first level production which is in -492 m and mining three groups of coal A, B, and C. The strata in the minefield area are deposited successively from top to bottom in Quaternary, Tertiary, Permian, Carboniferous, Ordovician, and Cambrian, and the mined coal are hosted in Permian. Most of the faults in Zhangji mining area are normal faults, and the strike is mainly NE-trending. The more developed faults will affect the continuous advance of mining face. Mine aquifer consists of Cenozoic loose pore aquifer, Permian sandstone fissure aquifer, and limestone karst fissure aquifer.

The main water hazards in mine mining are limestone water, goaf water, coal measures sandstone fissure water, and Cenozoic loose bed water, among which limestone water is the main threat source of 1# coal mining. Coal mining is directly threatened by the Carboniferous limestone aquifer on the floor. Ordovician limestone aquifer generally does not pose a direct threat to coal mining, but it can indirectly threaten through water conducting faults and hidden subsidence pillars.

2.2. Potential Danger of Water Inrush in Stope Floor. The average thickness of aquiclude in floor is about 17 m. Limestone confined aquifer is an important water source for mining. According to the multiple faults exposed in the driving roadway, dripping may occur in the mining face. It is necessary to take targeted water control measures under the influence of mining disturbance. And in April 2018, 11# orientated long borehole of -600 m drainage roadway in coal mining area appeared water gushing at 330 m depth. The initial water volume was about 3 m³/h. After all the drill pipes were pulled out, the stable water volume was 220 m³/h, and the water temperature was 40.5°. In order to further ensure the safety of mining, surface high-power time-frequency electromagnetic exploration and three-dimensional seismic

exploration are used to interpret and refine strata in the mining area, as shown in Figure 2.

Sensitive seismic attributes of prestack depth migration profiles are detected. The area below the water outlet presents attributes anomaly, which reflects the poor continuity of strata and may contain geological anomaly bodies. Seismic multiattribute detection results are extracted by slicing along the bottom boundary of Taihu gray. There is an elliptical maximum negative curvature property anomaly area near the outlet point. The low-value anomaly of minimum coherence presents “X” banded intersection, suspicious of conjugate shear faults. Combined with the results of borehole exploration, it is concluded that the anomaly body is a fault fracture zone, and there may be local stratum subsidence near the fault intersection point. The elliptical bad geological body is about 53 m in length and 35 m in width. Therefore, it is necessary to carry out grouting projects in the region and reinforce water shutoff and hydrophobic depressurization to reduce the risk of water inrush in fractured fault zones.

2.3. Grouting Process. The grouting process mainly relies on the ground grouting station to inject cement slurry into the stratum, as shown in Figure 3. The water-cement ratio will change the characteristics of cement [21], so the appropriate water-cement ratio slurry should be selected on site. The maximum diameter of grouting hole is 350 mm, with an average of 250 mm. The grouting material is ordinary Portland cement of water-cement ratio 1.2~1.7 without early setting agent. According to the previous research conclusions, the principles of small after first high ratio and combined continuous and intermittent grouting were followed in this grouting engineering. The grouting methods of stop slurry at injection orifice, subsection downward of horizontal branch holes or forward grouting, are adopted.

3. Methodology

When coal and other mineral resources are exploited, the water-bearing working faces cause easily inrush disaster through permeable passage in rock stope, a result from the geological faults and structural planes. When grouting is used to block the water in the fault fracture zone, the slurry often spread with two forms: (1) porous medium: in the area where rock is seriously broken, the slurry will flow with an approximate spherical diffusion mode under the external pressure, as shown in Figure 4(b); and (2) plane fracture: limited by the rock walls, approximate radial diffusion centered on grouting holes will occur in the main structural planes or permeable passages [39], as shown in Figure 4(a). In order to simplify the research and improve the universality of engineering requirements, complex engineering problems are generally transformed into 2D simplified models, which have better representativeness [40]. So, the grouting engineering can be simplified into a 2D model, as shown in Figure 4(c).

Grouting water plugging is a diffusion process of ground-water displacement in fissures, which is usually filled with water during plugging and reinforcement engineering. Slurry has a hindrance reaction from groundwater when flowing. In

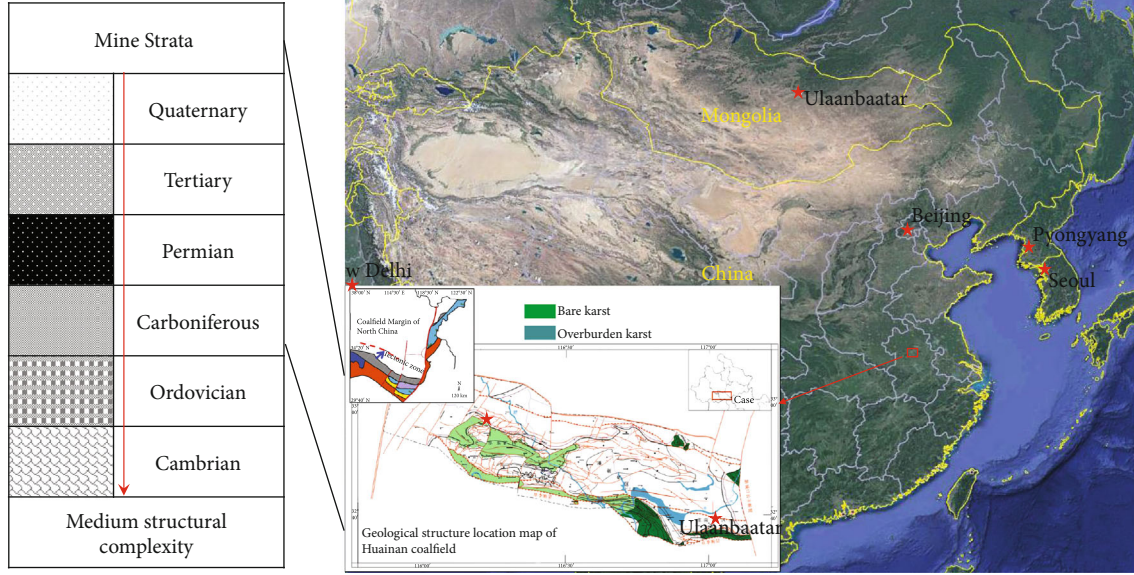


FIGURE 1: Schematic diagram of mining stope and generalized stratigraphic.

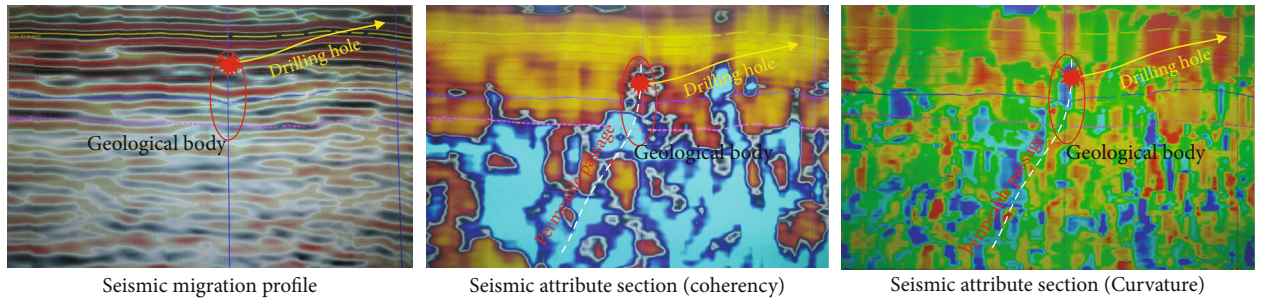


FIGURE 2: Seismic multiattribute analysis section.

the case of ignoring other factors, the slurry after completely mixing can be assumed to be a single-phase flow. Grouting engineering affected by water gushing essentially shows a slurry-water two-phase flow.

3.1. Radial Flow of Slurry. The slurry flow in fractures is governed by the mass and momentum balance equations. Based on NS equation, govern equations of single-phase in fracture can be given as follows [29, 41, 42]:

$$\begin{cases} \frac{\partial \rho_s}{\partial t} + \nabla \cdot (\rho_s \mathbf{u}_s) = 0 \\ \rho_s \frac{\partial \mathbf{u}_s}{\partial t} + \rho_s (\mathbf{u}_s \cdot \nabla) \mathbf{u}_s = -\nabla \mathbf{P}_s - \Delta \cdot \boldsymbol{\tau}_s + \mathbf{F}_g, \end{cases} \quad (1)$$

where ρ_s is the slurry density, t is the time, \mathbf{u}_s is the flow velocity, \mathbf{P}_s is the pressure, $\boldsymbol{\tau}_s$ is the shear stress, and \mathbf{F}_g is the gravitational stress. Chemical material such as polyurethane can be modeled by Newtonian fluids. The shear stress

can be given by several types, as illustrated:

$$\left. \begin{cases} \tau_{ij} = m \mu_s \dot{\gamma}_{ij}^{n-1}, \text{ Power Law fluids} \\ |\tau_{ij}| = \tau_0, |\tau_{ij}| \leq \tau_0 \\ \tau_{ij} = \left(\frac{\tau_0}{|\dot{\gamma}_{ij}|} + \mu_s \right) \dot{\gamma}_{ij}, |\tau_{ij}| > \tau_0 \\ \tau_{ij} = \mu_s \dot{\gamma}_{ij}, \text{ Newtonian fluids,} \end{cases} \right\}, \text{ Bingham fluids} \quad (2)$$

where τ_{ij} is the shear stress tensor, m is the power-law coefficient, μ_s is the slurry viscosity, n is the power-law index, τ_0 is the yield shear stress, and $\dot{\gamma}_{ij}$ is the shear rate which can be obtained by

$$\dot{\gamma}_{ij} = \nabla \mathbf{u}_s + (\nabla \mathbf{u}_s)^T. \quad (3)$$

Based on the $w/c = 1 \sim 1.5$ commonly used in

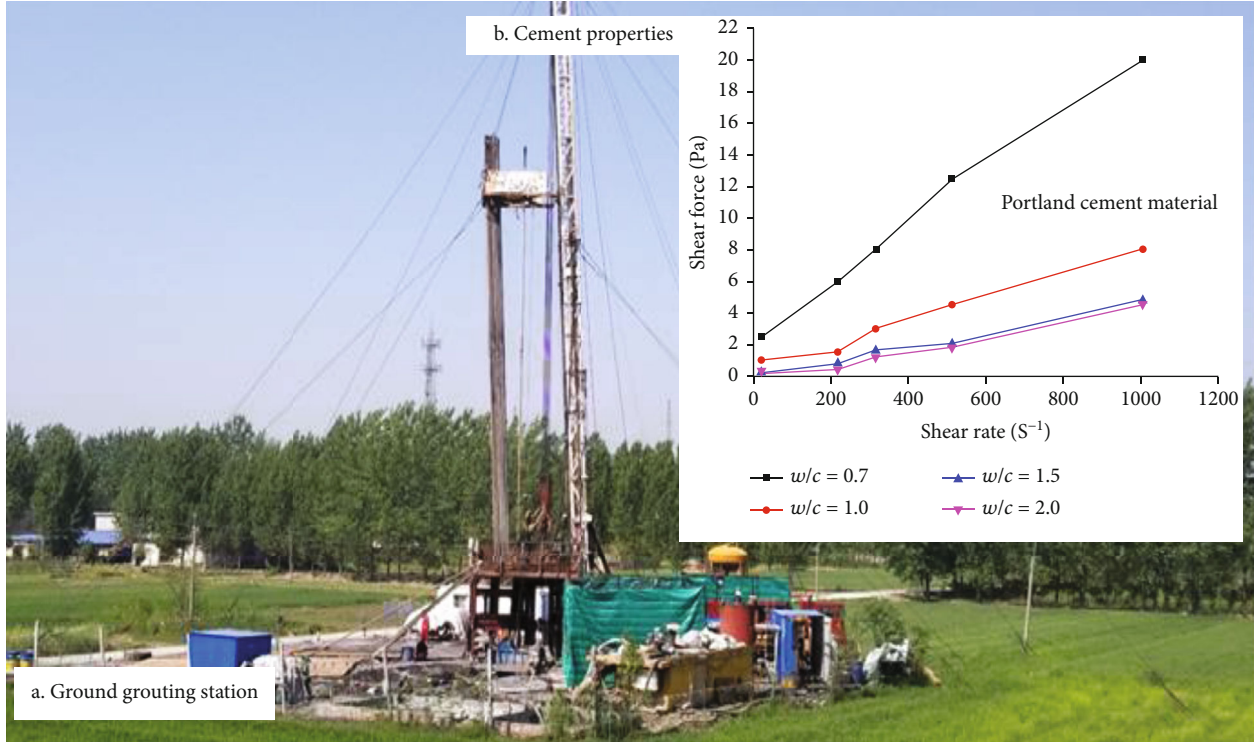


FIGURE 3: Grouting station and material [21].

engineering and to make the calculation simplify, there are also some assumptions:

- (1) The slurry and groundwater are both Newtonian fluids and incompressible
- (2) The gravitational forces and inertial effects are negligible
- (3) The path aperture is much smaller than lateral dimensions.

The mass equations for the single-phase of a Newtonian fluid flow in a homogenous fracture can be simplified as

$$\nabla \cdot \mathbf{u} = 0. \quad (4)$$

3.2. Two-Phase Flow. Grouting process involves immiscible two fluids of slurry and groundwater in the fracture. The external conditions in the radial direction of fracture during grouting have changed to be enclosed by water. There is an interface between them in displacement flow, which can be tracked by a phase transport equation. The level set method can be used to track the interface [38], and an interface equation can be given as follows:

$$\frac{\partial \phi}{\partial t} + \mathbf{u}_i \cdot \nabla \phi = \gamma \nabla \cdot \left(\varepsilon \nabla \phi - \phi(1 - \phi) \frac{\nabla \phi}{|\nabla \phi|} \right), \quad (5)$$

where ϕ is the level function, γ is the reinitialization parameter, and ε is the interface thickness controlling parameter.

The govern equations of the two-phase flow can be given by Eq. (6).

$$\begin{cases} \nabla \cdot \mathbf{u} = 0 \\ \rho \frac{\partial \mathbf{u}}{\partial t} + \rho(\mathbf{u} \cdot \nabla) \mathbf{u} = -\nabla \mathbf{P} - \Delta \cdot \boldsymbol{\tau} + \mathbf{F} + \mathbf{F}_{st} + \mathbf{F}_v \\ \boldsymbol{\tau} = \mu(\nabla \mathbf{u} + \nabla \mathbf{u}^T), \end{cases} \quad (6)$$

where \mathbf{F}_v is the volume force, ρ is the density, μ is the viscosity, and \mathbf{F}_{st} is the surface tension force which can be given by Eq. (7).

$$\begin{cases} \rho = \rho_1 + (\rho_2 - \rho_1)\phi \\ \mu = \mu_1 + (\mu_2 - \mu_1)\phi \\ \mathbf{F}_{st} = \nabla \cdot (\sigma(\mathbf{I} - (\mathbf{n}\mathbf{n}^T))6|\nabla \phi| |\phi(1 - \phi)|), \end{cases} \quad (7)$$

where σ is the surface tensions coefficient and \mathbf{n} is the unit normal to the interface.

3.3. Groundwater in the Fracture. The permeable formation in underground coal mining can generally be divided into goaf water, surface water, confined water, etc., and floor water inrush disaster is easily caused by confined water. In China, floor limestone water is a key issue of mining control, especially for stopes with permeable passage such as faults. Under the stratum high pressure, water flows into the working face through fissures or potential geological bodies. That is to say, the crack is filled with water with velocity and

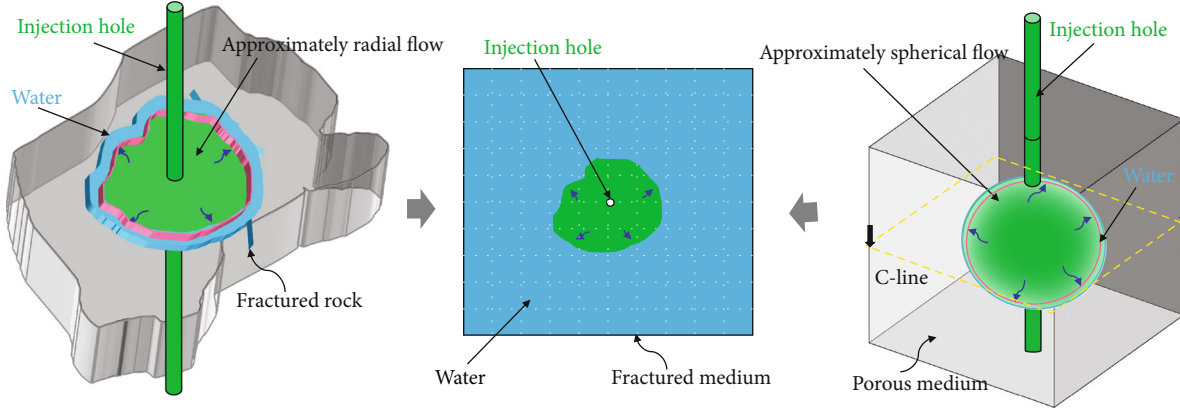


FIGURE 4: Schematic diagram of rock grouting.

pressure. From the initial stage, grouting displaces groundwater flow and bears its reaction. The pressure gradient and flowrate are given by Eq. (8).

$$\begin{cases} \frac{\partial p_i}{\partial x} = \frac{P_w - P_i}{L_i}, |P_w| < |P_i| \\ 0, \text{ otherwise} \\ \mathbf{u} > \mathbf{u}_w, \end{cases} \quad (8)$$

where P_w is the groundwater pressure, P_i is the grouting pressure, and L_i is the spread radius.

The grouting pressure should be larger than the groundwater pressure to spread. When the grouting pressure or velocity is less than groundwater, 0 distance flow will occur in the direction of reverse diffusion, resulting in grouting failure or even water inrush accident. Therefore, the magnitude and direction of groundwater hydraulic parameters must be considered during grouting water plugging, which is an important parameter affecting diffusion.

4. Results

4.1. Grouting Calculation. The calculation of fluid can be carried out by some software, and COMSOL software can be used in the field of multifield-coupling calculation, which covers fluid flow, heat conduction, structural mechanics, and other physical fields. The flow and diffusion can be calculated based on flow equation and coupling equation in a computational fluid dynamics (CFD) module.

According to the previous studies, the model can be simplified as a two-dimensional model, as shown in Figure 5. So, the grouting diffusion model is established in COMSOL, which has two kinds of boundaries of the hole boundary in the middle and open boundary on the four sides, and the middle boundary has null element formed by Boolean operation indicated as the grouting hole. The region between the two boundaries is the computational domain of fluid diffusion Ω . The fluid domain is divided into 15525 elements, and the near-boundary area of grouting hole is densified. The injection hole is the inlet of the slurry in the model cal-

ulation: the flow rate of slurry v_s , viscosity of slurry μ_s , and density of slurry ρ_s . The side boundary is the outlet: the out-pressure $P = 0$. The initial fluid domain contains flowing water: the flow rate of water v_w , viscosity of water μ_w , and density of water ρ_w . According to the calculation principle of two-phase flow, the initial region is water flow, which is fluid-1 by default; the slurry flowing into the flow region from the grouting hole is fluid-2. The interface between the two fluids can be traced by the volume ratio and pressure of fluid-2 to realize the time-varying characteristics of the dynamic diffusion trace.

4.1.1. The Effects of Flowing Water. To characterize the influence of water flow change on grouting diffusion, numerical simulation analysis is made on the slurry diffusion interface under two conditions (no water flow and with water flow), as shown in Figure 6. By comparison, the results show that the diffusion radius of slurry is R_t in any direction with time without the influence of water flow, which presents a standard disk diffusion model. As time goes on from T1, T2, to T3, the diffusion radius changes uniformly, which is consistent with the experimental results, as shown in the first one in Figure 6(c). When the diffusion of grouting is affected by hydrodynamic conditions, the diffusion state of grouting in each direction is obviously different. First of all, it is no longer the symmetry destruction with the grouting hole as the center in the X direction, but two kinds of diffusion radius $R_{t3} > R_{t1}$ with the grouting hole as the center are presented. And the difference between the two increased with time. At the same time, it can be found that the diffusion radius R_{t1} does not change with time in the upstream direction. Taking the grouting hole as the boundary (Y direction), there is an obvious blank zone of grouting slurry diffusion on the counter-current side. However, in the downstream direction, the diffusion has been completed at T3. In the Y direction, the maximum diffusion radius $R_{t2 \max}$ of slurry diffusion radius R_{t2} in the initial state is basically symmetrical with the grouting hole as the center. As time goes on to T2, the diffusion radius around the grouting hole does not increase significantly. But the maximum diffusion radius $R_{t2 \max}$ moves along the flow direction with the diffusion, which makes

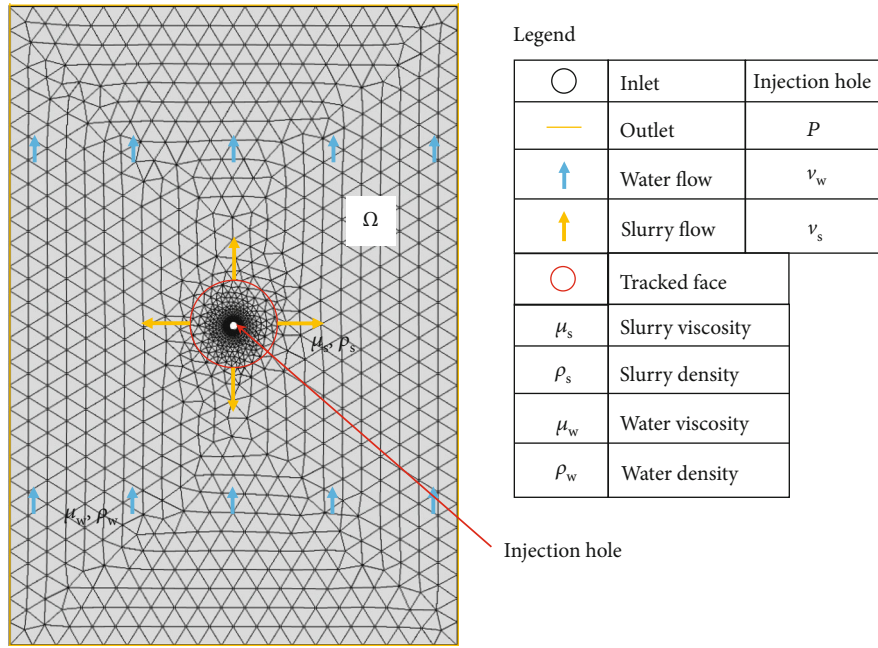


FIGURE 5: Calculation model.

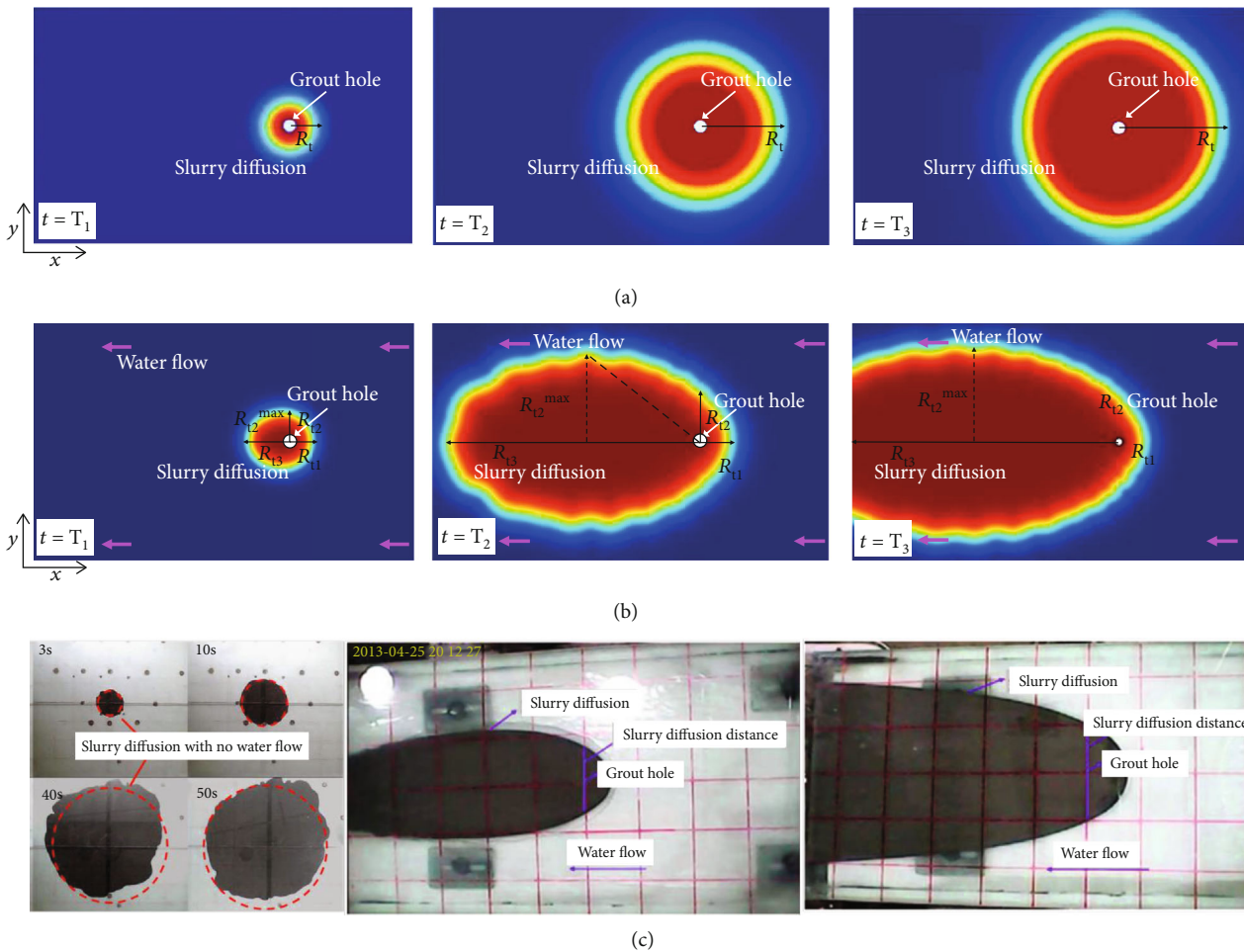


FIGURE 6: Numerical calculation and experimental verification of slurry diffusion. (a) Simulation of no water flowing. (b) Simulation of water flowing. (c) Experiment of slurry diffusion [43, 44].

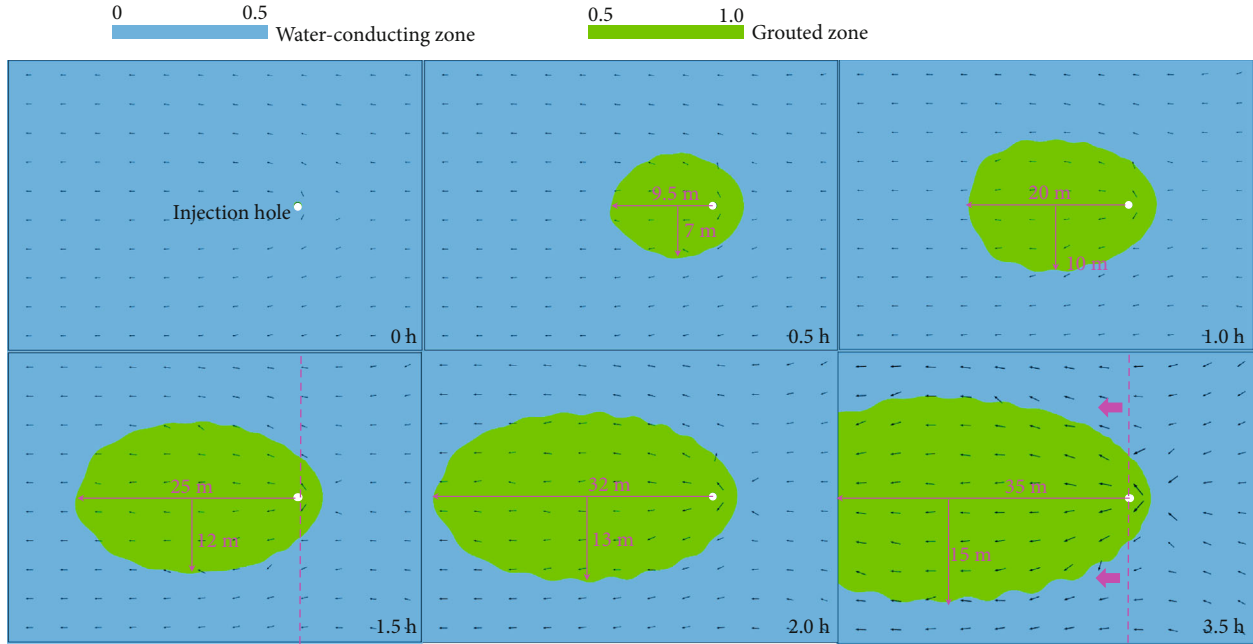


FIGURE 7: Diffusion boundary tracking from volume fraction.

the slurry diffusion state oval diffusion. In the Y direction near the boundary region, there is a symmetric diffusion white band. At T3, the maximum diffusion radius in Y direction is no longer obvious. When the slurry first diffuses to the boundary in the X direction, the slurry expands from the X boundary to the Y direction, and the blank band in the Y direction begins to fill gradually from the boundary.

At the same time, in order to verify the rationality of the simulation results, the previous research results are selected to verify. By comparing the previous experimental results, it can be found that the results calculated by the two-phase flow theory are consistent with the experimental results, as shown in Figure 6(c). Then it further shows that there are significant differences in the diffusion process and diffusion form of slurry under the condition of nonflowing water and flowing water. The time-varying model of two-phase flow can be used to simulate the slurry diffusion and its time-varying process.

4.1.2. Diffusion Trace from Volume Fraction in the Case. According to the design of grouting engineering, the water-cement ratio of cement slurry is from 0.8:1 to 1.5:1, and the hydraulic characteristics of this kind of slurry are Newtonian type. It is assumed that the slurry diffuses around a single-slab fracture and displaces the water flow. The setting velocity of water flow is 0.004 m/s, and the grouting hole diameter is 0.35 m. When the average velocity of grouting slurry is 0.03 m/s and the water-cement ratio is 1:1, the density of grouting slurry is 1400 kg/m³. The average viscosity measured by the test is about 0.04 Pa·s. In order to better represent the time-varying characteristics of cement slurry in the computational domain, the real-time range of 50%-100% proportion of fluid 2 (cement) is selected to characterize its diffusion, and the results are shown in Figure 7. Within 0.5 h of the diffusion calculation, there is little difference

between the diffusion trace along the flow direction and the two sides. At this time, the downstream diffusion distance is 9.5 m, and the maximum diffusion distance on both sides is about 7 m. At the time of 1 h, it has diffused about 20 m in the downstream direction, and the maximum diffusion distance on both sides is about 10 m. At 1.5 h, the downstream direction has spread more than 25 m, and the maximum diffusion distance on both sides is about 12 m. At 2.0 h, the downstream direction has spread more than 30 m, and the maximum diffusion distance on both sides is about 13 m. At the time of 3.5 h, the slurry has reached the left outlet boundary, and the diffusion calculation is transferred to both sides. At the same time, backflow will spread to most areas. In this process, the slurry increases rapidly along the flow direction, but there is no slurry diffusion in the reverse flow direction. In the diffusion zone on both sides of the downstream flow, the range of slurry increases slowly.

It can be seen from the numerical calculation that under the influence of groundwater flow, the diffusion radius of slurry basically reaches 30 m in about 3 hours, but it is only about 15 m on the side. The results show that there are great differences in the diffusion distance of the slurry in the fractures, and the leaf-type diffusion model takes the middle line of the grouting hole in the middle as the maximum diffusion distance. As time goes on, when the grouting slurry diffuses to the downstream boundary, the slurry begins to diffuse to the side. In the grouting region, affected by the water velocity, the slurry diffusion path is irregular, and there is basically no slurry on the upstream side of the grouting hole. In a considerable period of time, the diffusion range of slurry in a single hole is mainly along the flow direction, so it cannot be filled by slurry in the side and counter flow area. According to the interpretation of the geological case, the width of the structure is about 52 m. Therefore, diffusion can be achieved

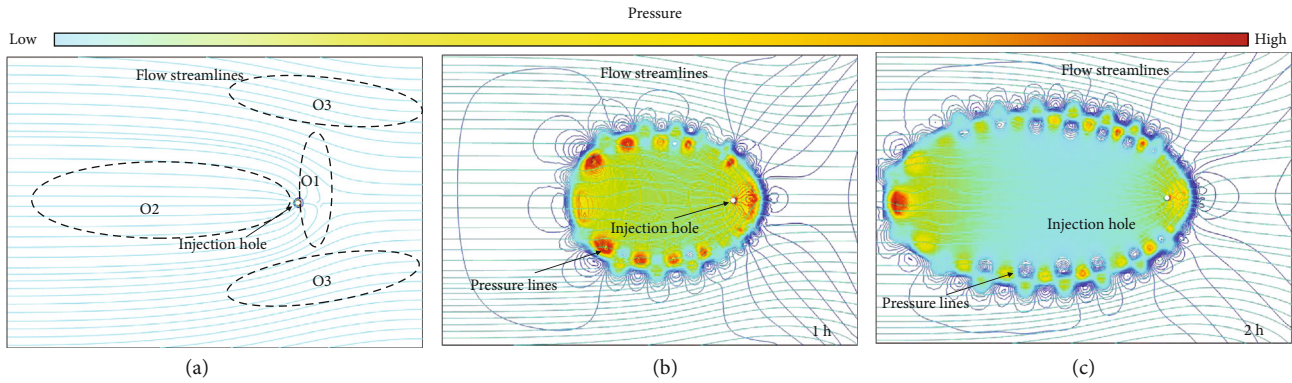


FIGURE 8: Grout pressure and streamlines in zone.

in the width direction, and three grouting holes can be established in the length direction to achieve the purpose of grouting water plugging and reinforcement.

4.1.3. Grout Pressure and Streamlines in Flow Zone. In order to clearly understand the interaction between water flow and slurry in the diffusion process, the absolute pressure and streamlines distribution are selected for calculation, and the results are shown in Figure 8. Affected by the constant velocity of the slurry in the grouting hole, the streamlines of the fluid can be divided into three distribution characteristics. In the O1 region, the streamlines are divergent, and there are typical arc corners and breakpoints. In the O2 region, the streamline extends from the grouting hole side to the left, which is generally the diffusion area of slurry. In the O3 region, the streamlines extend from the left initial end to the right, and deflects in the swept region of O1 region. These three stages reflect the change trend of the slurry and water in the process. It can be found that the reason for the slurry missing in the countercurrent area is that the streamlines are separated by the interface, as shown in Figure 8(a).

When the slurry fluid is injected into the flow field from the grouting hole, it will interfere with the original water pressure field and streamline field, as shown in Figures 8(b) and 8(c). When the displacement flow is continuously diffused after the slurry injection, the curvature direction of the streamline on the counter flow side will reverse, as shown in Figure 8(c), and the streamline grouting is compacted. At the same time, the pressure distribution in the downstream side of the grouting hole changes significantly with the diffusion of the slurry, while the pressure distribution in the upstream side does not change. There is a large fluid pressure field at the interface between slurry and water, and the envelope area of the larger pressure is the diffusion area of slurry. Therefore, the slurry-water interface is the boundary of maximum pressure distribution, and the slurry diffusion range can be characterized by the way of grout pressure in two-phase flow model.

4.2. Grouting Process Control

4.2.1. Optimization of Grouting Hole Design. Based on the slurry diffusion mechanism in the fracture with dynamic water in the engineering scale, if the single-hole grouting pro-

cess is implemented in the broken grouting area, the slurry diffusion distance is difficult to meet the grouting demand, so it is necessary to adopt the multihole and multisection grouting construction method. According to the numerical simulation results, when grouting is operated for a long time, there is obvious dominance in the direction of water flow. However, there are obvious grouting voids in the direction of upstream flow and both sides, so this feature should be considered when arranging grouting holes, as shown in Figure 9. When more than two grouting holes diffuse under water flow, the complexity of pregrouting area and the arc area of O1-O3 diffusion trace as shown in Figure 8(a) are considered. There is a slurry loss area in the arc corner intersection zone of the diffusion area, and the tip of the fracture area has the possibility of expanding upward and further penetrating.

Aiming at the regional diffusion problem caused by multiple grouting holes, the following optimization scheme is proposed:

- (a) All grouting holes should be arranged close to the intake side of water flowing to ensure that the required fracture zone is in the dominant diffusion area, and the slurry diffusion can cover all areas in the vertical direction, as shown in Figure 9(c)
- (b) In the area beyond the diffusion range of single-hole slurry, the second grouting hole is arranged on the premise of considering its diffusion radius in this direction, to ensure that the diffusion range of two grouting holes is crossed. Similarly, the third grouting hole is arranged to realize the full coverage of slurry in the whole area in this direction
- (c) Due to the influence of water flow on slurry diffusion, the layout of grouting holes does not adopt uniform height coordinate value in the direction of water flow but should present staggered layout in height, which can make one or two grouting holes produce larger grouting diffusion trace. The grouting area will cover the missing area of arc slurry
- (d) For the last grouting hole, due to the previous grouting hole having completed part of the crack plugging, it shows wide expansion under the effect of low water

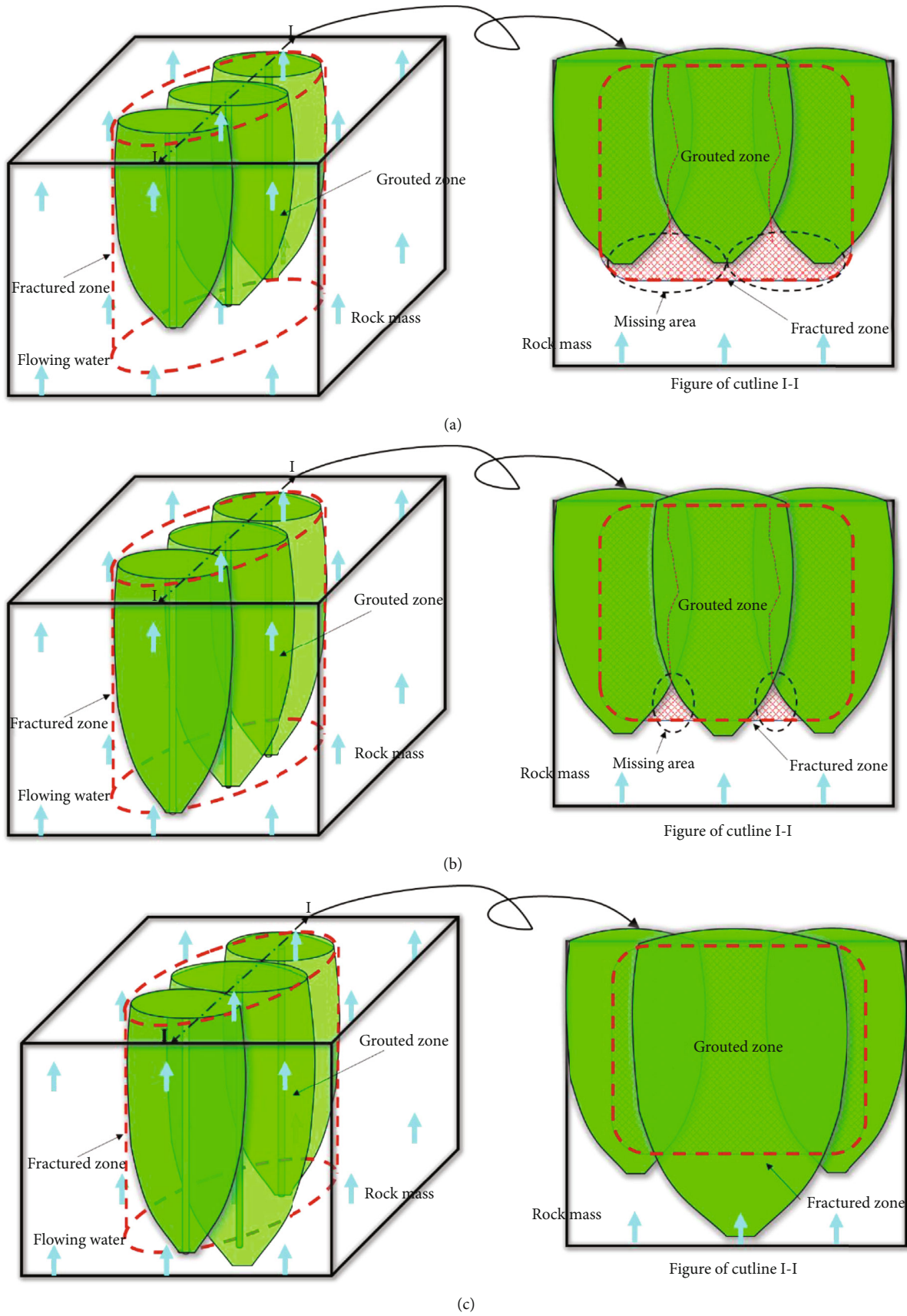


FIGURE 9: Slurry diffusion under different designs of grouting holes. (a) Slurry diffusion of drilling hole at side of noninlet water. (b) Slurry diffusion of drilling hole at side of inlet water with same level. (c) Slurry diffusion of drilling hole at side of inlet water with different levels.

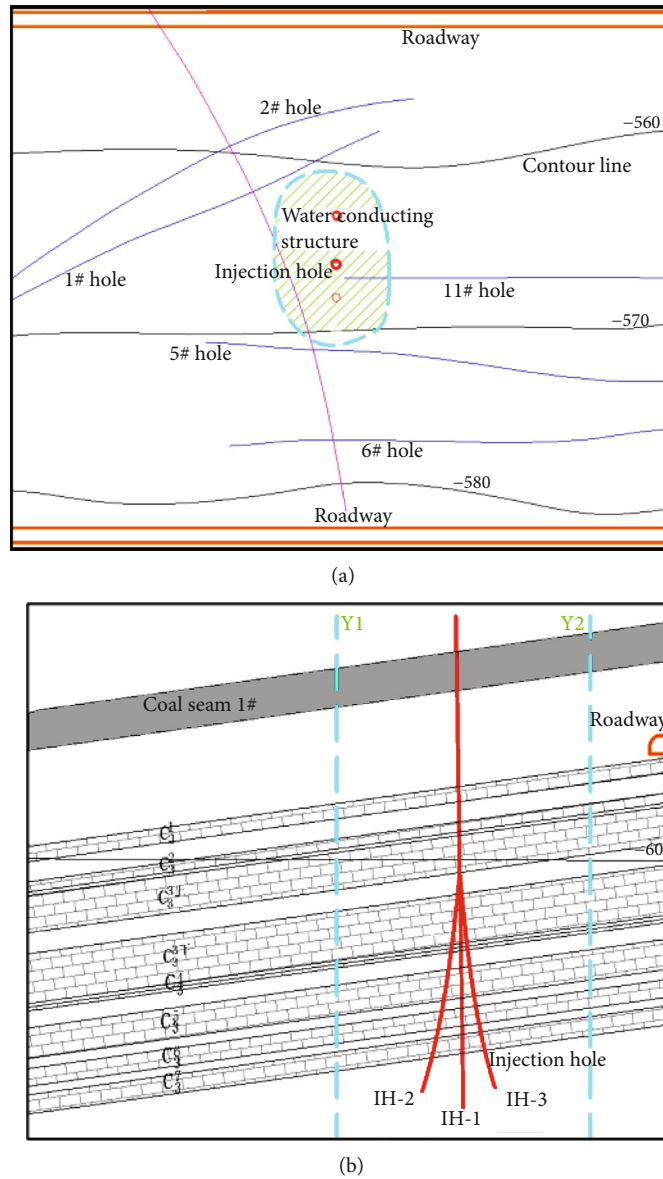


FIGURE 10: Grout holes in engineering. (a) Grouting plane diagram. (b) Grouting section diagram.

flow velocity; then the deep leakage filling grouting can be completed, as shown in Figure 9(c).

4.2.2. *Grouting Engineering.* According to the simulation results, considering the geological distribution in the dangerous area, the length and width in the plane are about 52 m and 30 m, and the grouting was carried out to plugging the water conducting structure (Y1~Y2 in Figure 10(b)). Three grouting holes are arranged on the long side for grouting construction, as shown in Figure 10(a). The range of slurry diffusion should exceed 52 m in length and 30 m in width. Among them, the main hole IH-1 is located in the middle of the concealed water channel, and the control range is $C_3^{3-1} \sim C_3^{11}$ (-694 m). The grouting hole IH-2 is located in the north of the main hole, and the depth range is C_3^9 (-655 m). The grouting hole IH-3 is located in the south of

the main hole, and the depth range is $C_3^6 \sim C_3^9$, as shown in Figure 10(b). Each borehole is staggered in spatial position.

According to the previous flow mechanism of cement slurry in cracks, the disadvantages of narrow cracks under low-pressure grouting and the distribution characteristics of diffusion range under dynamic water condition, the grouting is injected by stages in space. Firstly, the main hole (IH-2) is used to continuously inject cement into the formation, and the expected grouting effect is shown in Figure 9. Then, the grouting hole IH-3 is used to inject the slurry into the deep strata, and at the same time, it plays the role of sealing the nondiffused cracks in IH-2. Finally, the grouting hole IH-1 is used to inject liquid into limestone 11# to expand the diffusion range of cement near the working face and enhance the strength and tightness of rock stratum. According to the results of numerical simulation, each borehole in its

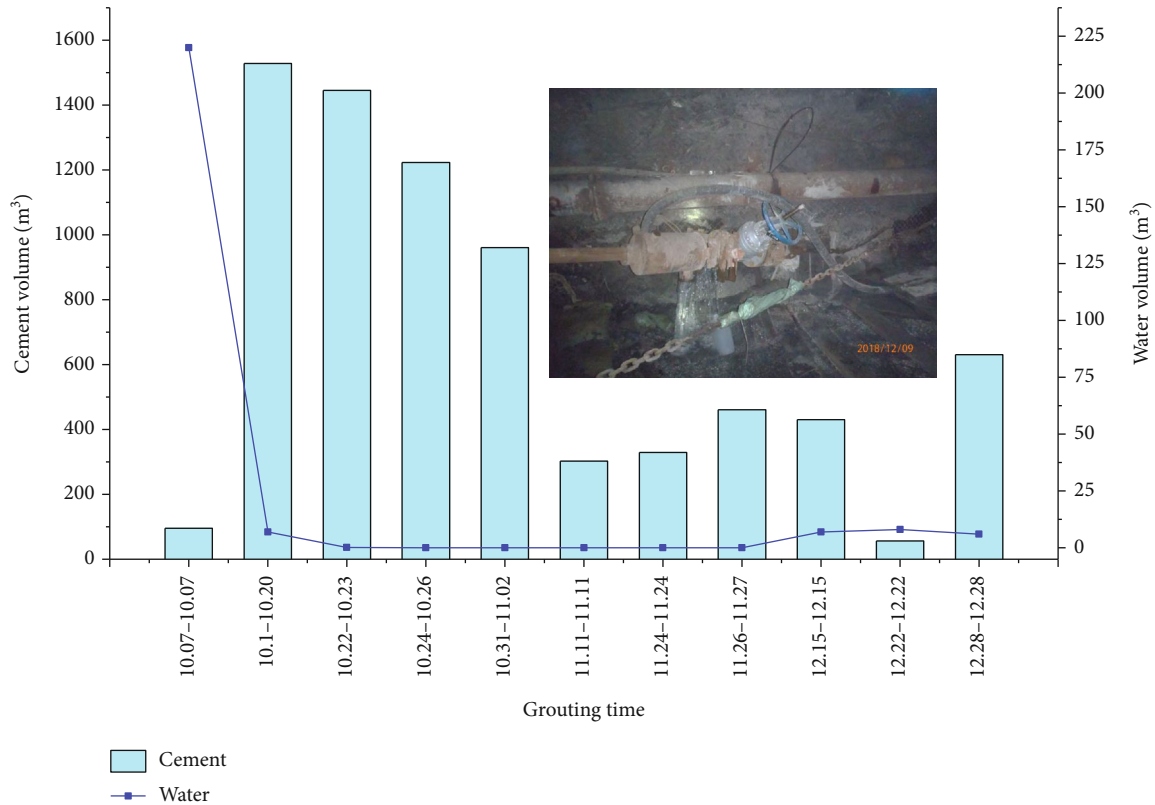


FIGURE 11: Grout cement and water seepage.

control area through continuous injection for more than 2 hours to achieve a predetermined diffusion range. At the same time, the main hole is used to seal the crushing area at the top by sections, and the water plugging effect is added.

4.3. Verification of Grouting Effect and Water Control. In the -600 m ash drainage roadway of West No.3 mining area of Zhangji mine, the water level of 11# hole of directional long borehole is C_3^3 lower limestone. The water source of the effluent is Ordovician limestone water. Therefore, the treatment target layer is determined as $C_3^3 \sim C_3^{11}$ ash to block the water outlet channel. If the water output of the verification hole is less than $3 \text{ m}^3/\text{h}$, it indicates that the grouting effect is feasible. The distributions of the primary and secondary faults and cracks were obtained from a geological survey based on the connectivity of grouting holes; the drilling holes were proposed and implemented from 10.08. The effective sealing of the floor water was realized after a regional sectional closed grouting. A segmental sealing grouting method (seven segments) was adopted to deal with the hydrophobicity of the floor. The real-time observations of hole H-11# revealed that the water inflow decreased to $7 \text{ m}^3/\text{h}$ after the third grouting, and then continued to decrease to 0, as shown in Figure 11. To further verify the effect of the grouting scheme, several checking holes were arranged in the upper section of the grouting in the fractured zone, such as TH-1#. Based on Figure 11, with the repeated grouting, the water flow in test hole is maintained in a stable small value after some grouting (from 12.15).

After performing coring in the field tunnel, it was found that the grouting veins were widely distributed. The main cracks consisting of wide and narrow cracks were filled with cement and consolidated with crushed rock following a multistage grouting, as shown in Figure 12. Based on the research finding here, the principle can be explained as changing the diffusion of the cement grout in the superior and inferior cracks and filling the inferior cracks with grout to plug them to achieve the effect of plugging the crack water under the condition of a low water pressure. The directional long borehole in the roadway is 35 m away from the adjacent grouting branch hole. Many cement cuttings were found during the construction of long boreholes, which shows that the diffusion range of grouting is not less than 35 m.

5. Discussion

Based on this study, the effect of water flow plays an important role in the diffusion of slurry. Therefore, five groups of numerical experiments were designed to discuss the influence mechanism of water flow on slurry. In the numerical calculation, the default slurry inlet velocity is 0.03 m/s , and other properties are consistent with the research basis of this paper. The size of the calculation model is length \times width = $50 \text{ m} \times 36 \text{ m}$. The design scheme and the data obtained are illustrated in Table 1.

After processing the data, it can be found that with the increase of time, the water flow rate has a good promotion effect on the slurry along the flow direction in a certain

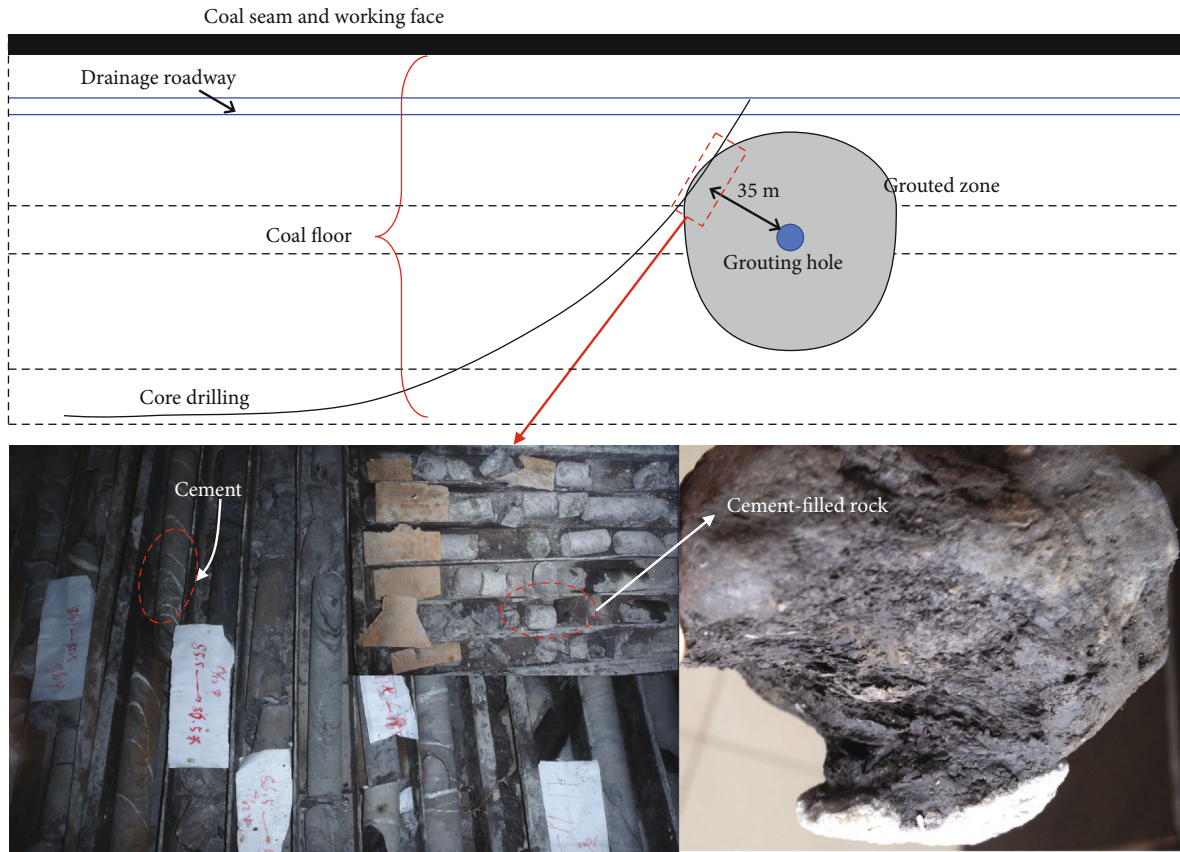


FIGURE 12: Core verification of grouting area in site.

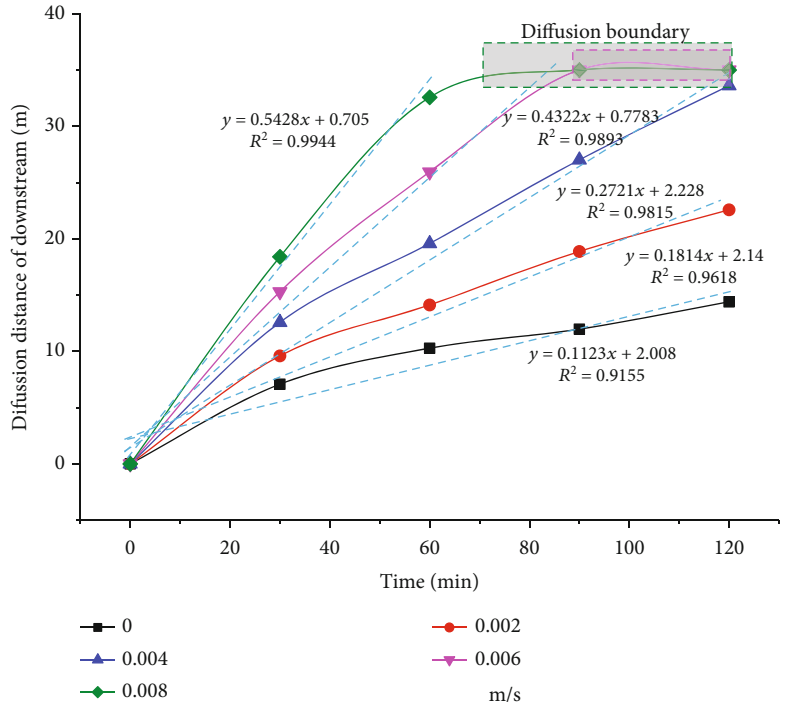
TABLE 1: Simulation parameters and results.

Water	0		0.002 m/s		0.004 m/s		0.006 m/s		0.008 m/s	
	Directions	Downstream	Side direction	Downstream	Side direction	Downstream	Side direction	Downstream	Side direction	
0 min	0	0	0	0	0	0	0	0	0	
30 min	7.08 m	9.59 m	6.88 m	12.58 m	6.55 m	15.3 m	6.18 m	18.4 m	5.71 m	
60 min	10.28 m	14.12 m	9 m	19.58 m	8.4 m	25.93 m	7.44 m	32.57 m	7 m	
90 min	11.97 m	18.87 m	10.8 m	27.01 m	9.57 m	35 m	8.33 m	35 m	7.39 m	
120 min	14.4 m	22.57 m	13.13 m	33.6 m	10.69 m	35 m	9.13 m	35 m	7.81 m	

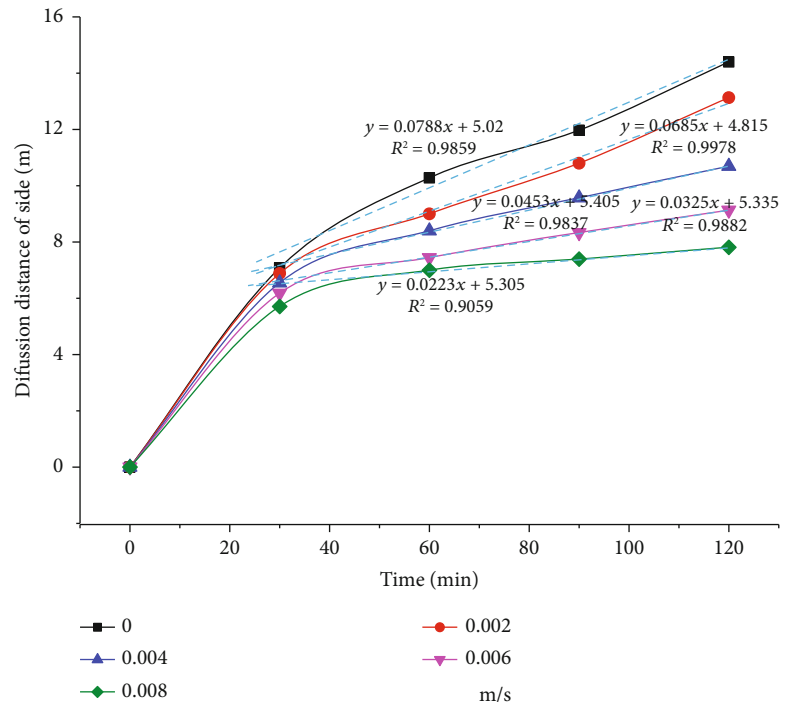
period, that is, it basically increases linearly, as shown in Figure 13(a). Moreover, in the model with high water velocity, the diffusion boundary will be reached first. We also know that [34] the water flow has a large scouring and dilution effect on the expansion of the slurry, which is not conducive to the sealing effect of the slurry on the cracks. Even in some cases, there will be leakage, misplaced grouting, and other accidents. At the same time, on the side of the grouting area, the diffusion range of the slurry increases slowly with time, as shown in Figure 13(b). The slurry growth slope in the range of slurry diffusion under different conditions was obtained. Through comparison, it can be found that the slope change rate increases linearly with the flow on the downstream side. However, the slurry diffusion rate on the side decreases linearly with the flow, as shown in Figures 13(c)

and 13(d). There are three different states of slurry under the influence of water flow: first, the increase of water velocity has a significant linear effect on the slurry diffusion along the water flow. Secondly, it has a linear inhibition effect on the side slurry diffusion. However, it has no effect on the reverse flow slurry. Therefore, it is very important to coordinate the relationship between water flow velocity and slurry diffusion, especially the advantage of water flow can be realized by modifying the grouting hole.

In the actual grouting operation, the influence of dynamic water is great. In addition to developing new grouting materials, the spatial relationship between grouting holes and rock fractures should be continuously optimized. Through the rational use of water flow, its negative impact on slurry diffusion seal should be reduced, and its positive

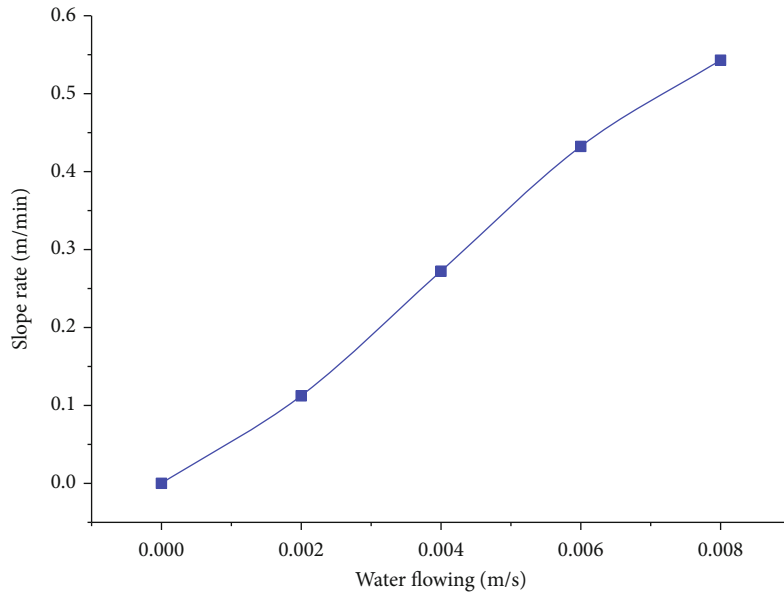


(a)

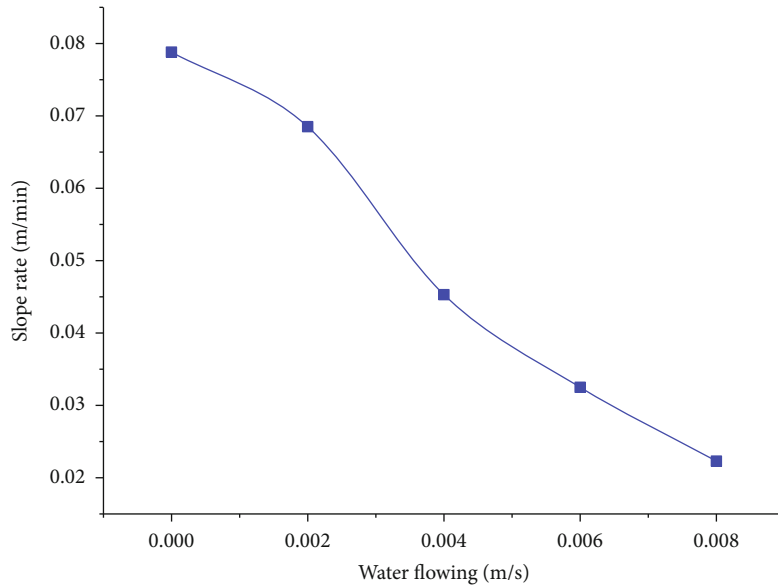


(b)

FIGURE 13: Continued.



(c)



(d)

FIGURE 13: Slurry diffusion characteristics under different flow conditions. (a) Slurry diffusion in downstream with time. (b) Slurry diffusion in side boundary. (c) Slope rate in downstream with water flowing. (d) Slope rate in upstream with water flowing.

role in slurry diffusion should be played. Especially for the energy production of coal mine, the generally used slurry is cement-based. So, the reasonable layout of grouting hole becomes a crucial factor under the condition of dynamic water. The research of this paper is aimed at this. The research was carried out based on the open boundary conditions of the model and the two-phase flow theory. However, in practical engineering applications, there are still significant fluid-structure interaction. For the influence of fluid-solid coupling, the future research work will focus on the diffusion mechanism of two-phase fluid-solid coupling slurry. The content of this study may be an important basis for the diffusion mechanism of grouting, and it is expected to play an important role in promoting the development of grouting

technology and the development and application of two-phase flow and fluid-solid coupling theory.

6. Conclusions

In this study, aiming at the problems of unclear diffusion mechanism and optimization of grouting process faced by grouting in broken area in engineering case, the grouting mechanism of slurry-water interface representing diffusion trace was studied based on two-phase flow theory, and the diffusion characteristics of slurry in dynamic water condition are revealed. The following can be concluded from the current study.

The conventional single-flow model based on NS equation is not accurate in predicting the diffusion range of slurry. Because of the external environment of flowing water in the grouting geological body, the interface characteristics and fluid properties of slurry and groundwater are different in the grouting process. The radial flow of slurry and fracture water flow can be used to establish equations for slurry and water flow, respectively. Considering the two-phase characteristics at the interface, the two-phase flow calculation model is established, and the level set method is used to track the interface between slurry and water. The diffusion range of slurry is characterized by 50%-100% volume ratio of slurry. Compared with the experimental results, the feasibility of two-phase flow study on slurry diffusion is verified.

Under the dynamic water environment, the diffusion form of slurry is changed due to the influence of water velocity, which is no longer a simple flat circular failure. Instead, it presents an "oval" or "leaf" diffusion mode with the grouting hole line as the axis, which develops to a "semioval" mode with the diffusion. There is no longer a standard diffusion radius, but different diffusion distances in all directions. There is a maximum diffusion distance along the flow direction, and it increases significantly with time. The diffusion distance on the side takes the second place and increases slowly with time. On the contrary, the diffusion range on the upstream side does not expand after a certain distance, and there is a large diffusion white belt.

Based on the data of grouting area measured by geophysical exploration in engineering case, the calculation model of slurry diffusion is established. According to the proportion of volume fraction, the diffusion shape and diffusion distance of slurry in different periods were analyzed. Under the proposed grouting rate, the grouting within the predetermined distance can be completed after continuous grouting for more than 3 hours, and the lateral diffusion distance was generally about 15 m. At the same time, the streamline distribution characteristics under the slurry-water interaction were analyzed, and the grouting pressure was used to characterize the slurry diffusion trace.

According to the diffusion mechanism of slurry and the distribution characteristics of void zone in single-hole grouting, the optimization scheme of grouting hole design was put forward, and the grouting mechanism was applied in the grouting case of Zhangji mine. The rationality and effectiveness of the grouting project were verified by the real-time monitoring of the water inflow in the area and the core drilling in the proposed grouting area. Furthermore, the correctness of grouting mechanism and optimization design under two-phase flow calculation was verified. The variation characteristics of slurry diffusion distance with different flow velocity, the grouting research, and technology optimization in the future dynamic water environment were discussed. The slurry diffusion mechanism under the two-phase flow coupling model will be further studied.

Data Availability

Data available on request.

Conflicts of Interest

The authors declare that they have no conflicts of interest.

Acknowledgments

This work was conducted with supports from the Anhui Natural Science Foundation (2008085ME145), National Science Foundation of China (Grant No. 51879041), the Central Government of Anhui Province Guided Local Development Projects (2019b12030027), and Anhui Science & Technology Specific Projects (17030901023).

References

- [1] W. Y. Guo, T. B. Zhao, Y. L. Tan, F. H. Yu, S. C. Hu, and F. Q. Yang, "Progressive mitigation method of rock bursts under complicated geological conditions," *International Journal of Rock Mechanics and Mining Sciences*, vol. 96, pp. 11–22, 2017.
- [2] S. C. Zhang, B. T. Shen, Y. Y. Li, and S. F. Zhou, "Modeling rock fracture propagation and water inrush mechanisms in underground coal mine," *Geofluids*, vol. 2019, Article ID 1796965, 15 pages, 2019.
- [3] W. Y. Guo, Q. H. Gu, Y. L. TAN, and S. C. Hu, "Case studies of rock bursts in tectonic areas with facies change," *Energies*, vol. 12, no. 7, p. 1330, 2019.
- [4] C. Zhu, X. D. Xu, X. T. Wang et al., "Experimental investigation on nonlinear flow anisotropy behavior in fracture media," *Geofluids*, vol. 2019, Article ID 5874849, 9 pages, 2019.
- [5] C. Zhu, Z. G. Tao, S. Yang, and S. Zhao, "V shaped gully method for controlling rockfall on high-steep slopes in China," *Bulletin of Engineering Geology and the Environment*, vol. 78, no. 4, pp. 2731–2747, 2019.
- [6] W. Q. Mu, L. C. Li, D. Z. Chen, S. X. Wang, and F. K. Xiao, "Long-term deformation and control structure of rheological tunnels based on numerical simulation and on-site monitoring," *Engineering Failure Analysis*, vol. 118, p. 104928, 2020.
- [7] X. Chang, Z. H. Li, S. Y. Wang, S. R. Wang, L. Fu, and C. A. Tang, "Pullout performances of grouted rockbolt systems with bond defects," *Rock Mechanics and Rock Engineering*, vol. 51, no. 3, pp. 861–871, 2018.
- [8] W. H. Baker, E. J. Cording, and H. H. MacPherson, *Compaction Grouting to Control Ground Movement during Tunneling. Underground Space*, Pergamon Press, New York, 1983.
- [9] H. Lisa, B. Christian, F. Asa, G. Gunnar, and F. Johan, "A hard rock tunnel case study: characterization of the water-bearing fracture system for tunnel grouting," *Tunnelling and Underground Space Technology*, vol. 30, pp. 132–144, 2012.
- [10] T. Zhao and C. Y. Liu, "Roof instability characteristics and pre-grouting of the roof caving zone in residual coal mining," *Journal of Geophysics and Engineering*, vol. 14, no. 6, pp. 1463–1474, 2017.
- [11] Z. Zheng, R. T. Liu, S. C. Li, and H. L. Yang, "Control of ground uplift based on flow-field regularity during grouting in fracture with flowing groundwater," *International Journal of Geomechanics*, vol. 20, no. 3, article 04020014, 2020.
- [12] M. El Tani and H. Stille, "Grout spread and injection period of silica solution and cement mix in rock fractures," *Rock Mechanics and Rock Engineering*, vol. 50, no. 9, pp. 2365–2380, 2017.

- [13] J. P. Zuo, Z. J. Hong, Z. Q. Xiong, C. Wang, and H. Q. Song, "Influence of different W/C on the performances and hydration progress of dual liquid high water backfilling material," *Construction and Building Materials*, vol. 190, pp. 910–917, 2018.
- [14] J. P. Zhang, L. M. Liu, Q. H. Li et al., "Development of cement-based self-stress composite grouting material for reinforcing rock mass and engineering application," *Construction and Building Materials*, vol. 201, pp. 314–327, 2019.
- [15] W. Q. Mu, L. C. Li, T. H. Yang, L. J. Yao, and S. X. Wang, "Numerical calculation and multi-factor analysis of slurry diffusion in an inclined geological fracture," *Hydrogeology Journal*, vol. 28, no. 3, pp. 1107–1124, 2020.
- [16] A. Zolfaghari, A. S. Bidar, M. R. M. Javan, M. Haftani, and A. Mehinrad, "Evaluation of rock mass improvement due to cement grouting by Q-system at Bakhtiary dam site," *International Journal of Rock Mechanics and Mining Sciences*, vol. 74, pp. 38–44, 2015.
- [17] B. Amadei and W. Z. Savage, "An analytical solution for transient flow of Bingham viscoplastic materials in rock fractures," *International Journal of Rock Mechanics & Mining Sciences*, vol. 38, no. 2, pp. 285–296, 2001.
- [18] S. Zhang, W. G. Qiao, P. C. Chen, and K. Xi, "Rheological and mechanical properties of microfine-cement-based grouts mixed with microfine fly ash, colloidal nanosilica and superplasticizer," *Construction and Building Materials*, vol. 212, pp. 10–18, 2019.
- [19] W. Q. Mu, L. C. Li, X. G. Liu et al., "Diffusion-hydraulic properties of grouting geological rough fractures with power-law slurry," *Geomechanics and Engineering*, vol. 21, no. 4, pp. 357–369, 2020.
- [20] U. Håkansson, L. Hässler, and H. Stille, "Rheological properties of microfine cement grouts," *Tunnelling and Underground Space Technology*, vol. 7, no. 4, pp. 453–458, 1992.
- [21] Q. S. Liu, G. F. Lei, X. X. Peng, C. B. Li, and W. Li, "Rheological characteristics of cement grout and its effect on mechanical properties of a rock fracture," *Rock Mechanics and Rock Engineering*, vol. 51, no. 2, pp. 613–625, 2018.
- [22] J. Funehag and A. Fransson, "Sealing narrow fractures with a Newtonian fluid: model prediction for grouting verified by field study," *Tunnelling and Underground Space Technology*, vol. 21, no. 5, pp. 492–498, 2006.
- [23] M. J. Yang, Z. Q. Yue, P. K. K. Lee, B. Su, and L. G. Tham, "Prediction of grout penetration in fractured rocks by numerical simulation," *Canadian Geotechnical Journal*, vol. 39, no. 6, pp. 1384–1394, 2002.
- [24] Y. H. Jin, L. J. Han, C. Y. Xu, Q. B. Meng, Z. J. Liu, and Y. J. Zong, "Cement grout nonlinear flow behavior through the rough-walled fractures: an experimental study," *Geofluids*, vol. 2020, Article ID 9514691, 12 pages, 2020.
- [25] H. Shimada, A. Hamanaka, T. Sasaoka, and K. Matsui, "Behaviour of grouting material used for floor reinforcement in underground mines," *International Journal of Mining Reclamation and Environment*, vol. 28, no. 2, pp. 133–148, 2014.
- [26] G. Lombard, "The role of cohesion in cement grouting of rock (Q 58, R 13). In: 15th congress of large dams," *ICOLD Lausanne*, pp. 235–261, 1985.
- [27] J. Funehag and G. Gustafson, "Design of grouting with silica sol in hard rock - New methods for calculation of penetration length, Part I," *Tunnelling and Underground Space Technology*, vol. 23, no. 1, pp. 1–8, 2008.
- [28] J. Funehag and J. Thörn, "Radial penetration of cementitious grout - Laboratory verification of grout spread in a fracture model," *Tunnelling and Underground Space Technology*, vol. 72, pp. 228–232, 2018.
- [29] W. Q. Mu, L. C. Li, T. H. Yang, G. F. Yu, and Y. C. Han, "Numerical investigation on a grouting mechanism with slurry-rock coupling and shear displacement in a single rough fracture," *Bulletin of Engineering Geology and the Environment*, vol. 78, no. 8, pp. 6159–6177, 2019.
- [30] P. Yang, Y. H. Liu, S. W. Gao, and S. B. Xue, "Experimental investigation on the diffusion of carbon fibre composite grouts in rough fractures with flowing water," *Tunnelling and Underground Space Technology*, vol. 95, p. 103146, 2020.
- [31] W. H. Sui, J. Y. Liu, W. Hu, J. F. Qi, and K. Y. Zhan, "Experimental investigation on sealing efficiency of chemical grouting in rock fracture with flowing water," *Tunnelling and Underground Space Technology*, vol. 50, pp. 139–249, 2015.
- [32] P. Yang, T. B. Li, L. Song, T. Deng, and S. B. Xue, "Effect of different factors on propagation of carbon fiber composite cement grout in a fracture with flowing water," *Construction and Building Materials*, vol. 121, pp. 501–506, 2016.
- [33] P. Yang, Y. H. Liu, S. W. Gao, and Z. C. Li, "Experiment on sealing efficiency of carbon fiber composite grout under flowing conditions," *Construction and Building Materials*, vol. 182, pp. 43–51, 2018.
- [34] Y. H. Wang, P. Yang, Z. T. Li, S. J. Wu, and Z. X. Zhao, "Experimental-numerical investigation on grout diffusion and wash-out in rough rock fractures under flowing water," *Computers and Geotechnics*, vol. 126, p. 103717, 2020.
- [35] Y. X. Guo, Q. S. Zhang, F. Xiao, R. T. Liu, Z. J. Wang, and Y. K. Liu, "Grouting rock fractures under condition of flowing water," *Carbonates and Evaporites*, vol. 35, p. 96, 2020.
- [36] Y. H. Liu, P. Yang, Z. B. Yang, X. Wei, and L. S. Zhang, "Effect of Nano-CaCO₃ on the sealing efficiency of grouts in flowing water grouting," *KSCE Journal of Civil Engineering*, vol. 24, no. 10, pp. 2923–2930, 2020.
- [37] L. C. Zou, U. Håkansson, and V. Cvetkovic, "Two-phase cement grout propagation in homogeneous water-saturated rock fractures," *International Journal of Rock Mechanics and Mining Sciences*, vol. 106, pp. 243–249, 2018.
- [38] B. Lafaurie, C. Nardone, R. Scardovelli, S. Zaleski, and G. Zanetti, "Modelling merging and fragmentation in multiphase flows with SURFER," *Journal of Computational Physics*, vol. 113, no. 1, pp. 134–147, 1994.
- [39] M. El Tani, "Grouting rock fractures with cement grout," *Rock Mechanics and Rock Engineering*, vol. 45, no. 4, pp. 547–561, 2012.
- [40] S. Mohajerania, A. Baghbananb, G. Wangc, and S. F. Forouhandeh, "An efficient algorithm for simulating grout propagation in 2D discrete fracture networks," *International Journal of Rock Mechanics and Mining Sciences*, vol. 98, pp. 67–77, 2017.
- [41] T. Koyama, I. Neretnieks, and L. Jing, "A numerical study on differences in using Navier-Stokes and Reynolds equations for modeling the fluid flow and particle transport in single rock fractures with shear," *International Journal of Rock Mechanics and Mining Sciences*, vol. 45, no. 7, pp. 1082–1101, 2008.
- [42] L. Z. Xie, C. Gao, L. Ren, and C. B. Li, "Numerical investigation of geometrical and hydraulic properties in a single rock fracture during shear displacement with the Navier-Stokes equations," *Environmental Earth Sciences*, vol. 73, no. 11, pp. 7061–7074, 2015.

- [43] W. S. Yu, P. Li, X. Zhang, and Q. Wang, "Model test research on hydrodynamic grouting for single fracture with variable inclinations," *Rock and Soil Mechanics*, vol. 35, no. 8, pp. 2137–2149, 2014.
- [44] Q. S. Zhang, L. Z. Zhang, and R. T. Liu, "Grouting mechanism of quick setting slurry in rock fissure with consideration of viscosity variation with space," *Tunnelling and Underground Space Technology*, vol. 70, pp. 262–273, 2017.